ELEKTROPIKA: Int. J. of Electrical, Electronic Engineering and Technology, Vol. 1, 23–35, 2011

SEGMENTATION TECHNIQUE FOR ACUTE LEUKEMIA BLOOD CELLS IMAGES USING SATURATION COMPONENT AND MOVING K-MEAN CLUSTERING PROCEDURES

Nor Hazlyna Harun and Mohd Yusof Mashor

Electronic & Biomedical Intelligent Systems (EBItS) Research Group
School of Mechatronic Engineering, Universiti Malaysia Perlis
02600 Jejawi, Arau, Perlis, MALAYSIA
E-mail: hazlyna_harun@yahoo.com

Rosline Hassan

Hematology Department, University Hospital, Universiti Sains Malaysia
Kubang Kerian, Kelantan, MALAYSIA

Abstract—Image segmentation is the most important step and critical task in image processing as it will directly affect the post-processing. One of the common segmentation techniques is using clustering algorithm. Clustering technique is commonly used as a digital image segmentation including medical images. The current study proposes an automated color image segmentation using combination of saturation component of HSI color space, a Moving K-means clustering and 7×7 pixels median filter. In the proposed technique, saturation formula was applied to ease the segmentation process. After that, Moving K-means clustering was used to segment the blasts from acute leukemia blood images automatically. After the segmentation process has been completed, 7×7 pixels median filter was applied to eliminate and remove unwanted noise. To measure the efficiency of the proposed technique, pixel subtraction technique will be used. The results show that the proposed technique has successfully segmented and distinguished most of the acute leukemia blood cells from its background, while preserving significant features compared to the method based on a conventional K-means clustering algorithm.

Keywords: Segmentation, Acute leukemia, Blood cell images, Moving K-means clustering, Saturation formula and K-means clustering

1. INTRODUCTION

The term leukemia refers to a group of cancers of the blood cells which occurs when the cells stop working and functioning properly. In leukemia, white blood cells become abnormal, divide and grow in an uncontrolled way. Leukemia is divided into two main categories acute and chronic. Next, leukemia diseases further divided by the type of white blood cell, which affected myeloid or lymphoid. Leukemia is developed from the myeloid/granulocyte cell line is called acute myeloid leukemia (AML). Lymphocytic precursors give rise to acute lymphocytic leukemia (ALL) [1].

In February 2009, the World Health Organization (WHO) has reported the total death rate per 100,000 populations for leukemia carrier in the third world countries. It is estimated that in 2004 the number of death per 100,000 populations was 11.4 for Iraq, Afghanistan 8.4, Israel 7.6, Armenia 7.6, Turkey 6.2, Russia Federation 6.1, Jordon 5.9, Japan 5.7, Cyprus 5.2, Yemen 5.3, Cambodia 5.3, Sri Lanka 4.6, Maldives 4.4, Indonesia 4.4, Thailand 4.2 China 4.0 and Malaysia 0.9 [2]. According to the National Cancer Institute report, in 2009 for 17 SEER (Surveillance

Epidemiology and End Results) geographic areas, it is estimated that 5,330 men and women (3,150 men and 2,180 women) are diagnosed with leukemia and 1,420 men and women are predicted to die of ALL in 2010 [3]. Furthermore, from 2003-2007, the median age at diagnosis for ALL was 13 years of age. The statistic also estimated that 12,330 men and women (6,590 men and 5,740 women) are going to be diagnosed with AML and 8,950 men and women will die from AML in 2010. In between 2003-2007, the median age at diagnosis for AML was 67 years of age. The word acute means that, the disease develops and progress rapidly [4]. Acute leukemia tends to affect very young children or older adults. Acute leukemia has come on suddenly, often within days or weeks, progressing quickly and need to be treated urgently. Specific type of leukemia must be classified to provide the best treatment and most accurate prognosis [4].

The original classification scheme proposed by the French-American-British (FAB) Cooperative Group divided AML into 8 subtypes (M0 to M7) and ALL into 3 subtypes (L1 to L3). The FAB classification of ALL (L1 to L3) which is differentiated based on morphology, including cell size, prominence of nucleoli, and the amount and appearance of cytoplasm [1]. According to French-American-British (FAB) classification, the description of cells is small and uniform for ALL -L_1. Meanwhile, cells of AML-M_1 are large and regular [1]. Knowing the subtypes and classification of acute leukemia helps in predicting the clinical behavior of the disease and the prognosis, also in making treatment recommendations [5].

For the diagnosis of leukemia in laboratories, hematologists and technologists analyze human blood by microscope investigation. Unfortunately, the analysis made by experts (refer to medical persons) is not swift and the procedure is not standardized nor accurate due to the operator's capabilities and tiredness [6]. To improve the reliability of the diagnosis and decreasing the dependency on human experts, computer based digital image processing system is introduced for investigating and classifying acute leukemia diseases. The success of computer-aided classification of acute leukemia is closely dependent on the accurate segmentation of images [6].

Many segmentation methods for blood cell images have been proposed and developed. The common segmentation techniques used in cell segmentation are histogram thresholding, edge detection, region growing and clustering algorithm. Clustering algorithms is one of the most popular methods for segmentation techniques. Clustering algorithms can be applied in many fields for example statistics, computer science and machine learning [7]. Clustering algorithm is the method of organizing objects into categories, which members are similar in some way and dissimilar members belonging to other categories [7]. Currently, clustering algorithm such as K-means, Fuzzy K-means and Moving K-means have also been proved to produce good medical image segmentation performance [8, 9]. Wu et al. [10] used K-means clustering to track the tumor object in MRI brain image. Meanwhile, Etehad-Tavakol et al. [11] proposed K-means and Fuzzy K-means clustering, for color segmentation of the infrared thermal breast images. The problems related to conventional K-means are dead centre, pixels redundancy and trapped in local minima.

In 2000, Mashor [12] proposed a modified version of K-means clustering called Moving K-means in order to reduce the problems. Then, Mat-Isa et.al [13–15] claimed that Moving K-mean clustering is better in reducing dead centre, centre redundancy and trapped centre in local minima as compared to conventional K-means and Fuzzy K-means algorithm. Due to the ability of Moving K-means clustering technique, this study proposed a combination of saturation formula of HSI color space, Moving K-means algorithm and 7×7 pixels median filter to segment automatically the acute leukemia blood cells from its background and unwanted noise. The proposed automated color segmentation technique has been evaluated using pixels subtraction technique to measure the performance accuracy between conventional K-means and Moving K-means algorithm. The experimental results show that the proposed technique reveals the features of blasts cell in acute leukemia blood images such as shape and cells size. This information is important to distinguish either the blood images are AML or ALL for further analysis by hematologists.

2. METHODOLOGY

The goal of this proposed technique is to automate the segmentation process. The proposed technique consists of saturation formula, Moving K-means algorithm and 7×7 pixels median filter. Finally, the performance of the proposed technique has been evaluated by using pixels subtraction technique. The proposed technique involves the following key tasks:

2.1. Image Acquisition

The samples of acute leukemia blood slides have been provided by Hospital Universiti Sains Malaysia (HUSM). Then, the acute leukemia blood slides were analyzed using *Leica* microscope at 40X magnifications. After that, *Infinity 2* camera was used to capture the slide images and saved into (.bitmap) format at 800×600 resolution. In order to confirm the correctness of the blast cells in acute leukemia images the captured images have been revised and approved by hematologists. Figure 1 (a) and (b) are the examples of captured blood cell images consist of acute leukemia cells.

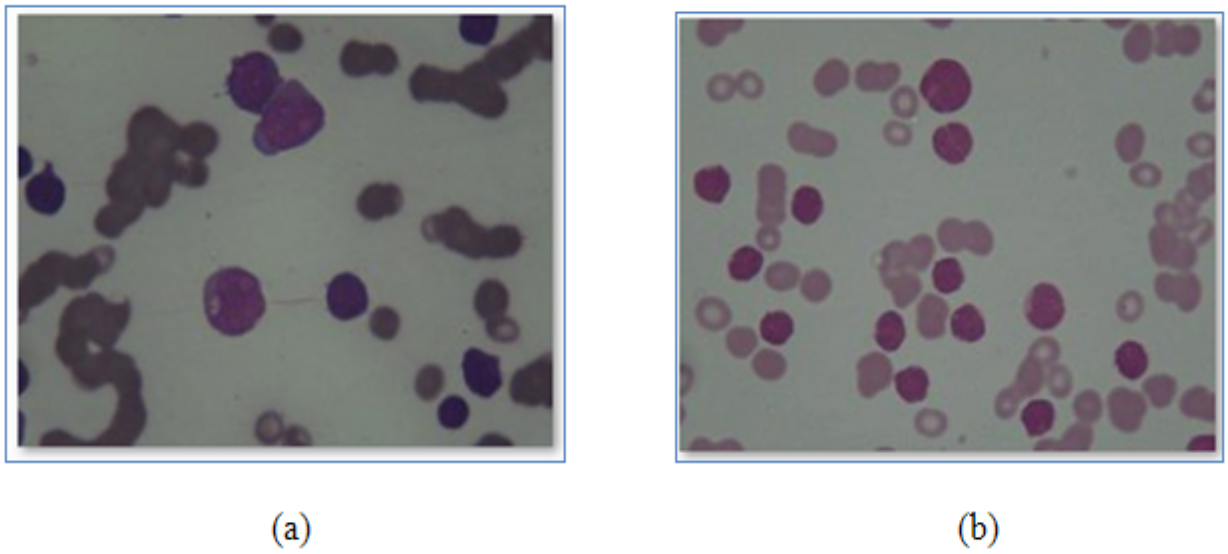

Figure 1: Sample of peripheral blood smear of acute leukemia patient containing (a)AML and (b)ALL blast cells

2.2. Threshold Selection Method

The threshold selection method consists of two steps. The proposed selection method will utilize saturation formula base on HSI color space. Then, the resultant image is used as the input for clustering algorithm. The steps are:

2.2.1. Saturation Component based on HSI Color Space

In [16] color image segmentation was conducted using RGB information of the acute leukemia blood cells image. However, the segmentation using manual RGB pixels threshold value did not perform well due to inconsistency of color in the images. The threshold value is selected based on the changes in the acute leukemia blood cells image. The reasons are subjected to the preparation of

staining procedure (operator dependent) and blood concentrations of individual. Therefore, another approach of segmentation using HSI color space is considered to reduce this problem. Figure 2 shows an example of acute leukemia blood cells and its HSI color component image.

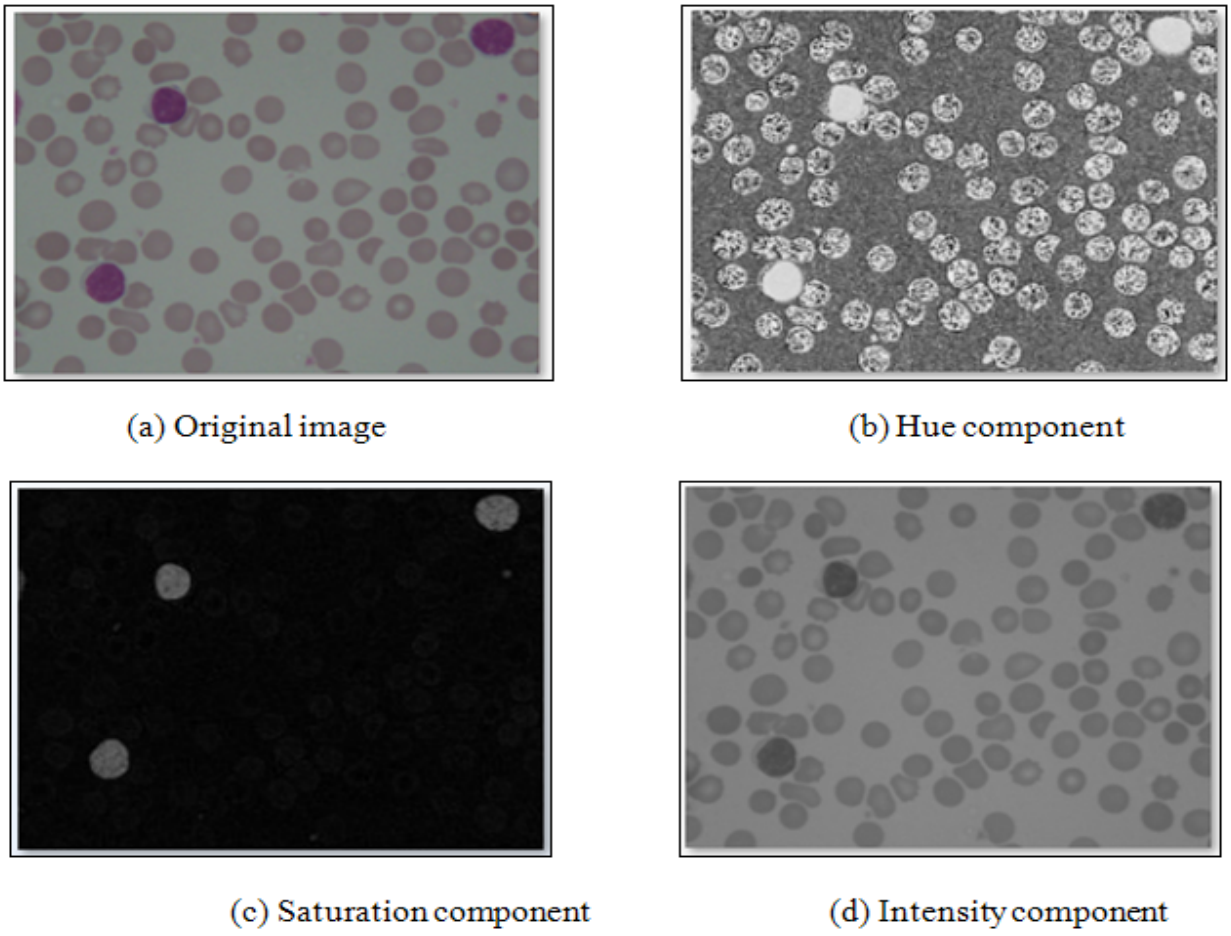

Figure 2: Acute Lymphoid Leukemia (ALL) blood cells image and its HSI color components

In general, the HSI color space consists of three components Hue, Saturation and Intensity. The saturation component measures the degree of white light added to pure color. Based on observation of blood cells image, the acute leukemia cells (blast) are the most highlighted and clearly seen in saturation component image. In contrast, the visibility of red blood cells and other particles become less in the saturation component image. Therefore, the saturation component is chosen in order to reduce the computational effort and to ease the clustering process. The saturation formula is applied to the original acute leukemia blood slide images as in (1).

$$Sat = 1 - \frac{3}{R+G+B} min\,(R, G, B) \tag{1}$$

After that, the resultant image will be used as the input to Moving K-means clustering. Detail descriptions of RGB to HSI and HSI to RGB transformation could be found in [17].

2.2.2. Moving K-means Clustering

The conventional K-mean clustering and Fuzzy K-mean clustering are widely used for automatic image segmentation [11]. However, both methods do not always produce a good result due to dead centre, centre redundancy and trapped in local minima. Mashor [12] proposed a modified k-mean clustering algorithm called Moving K-means clustering, in order to reduce these problems. The method was originally used for positioning the centre of radial basis function (RBF) network, but later found suitable for image segmentation [13,14,18]. Consider a problem that has N input pixels of image to be clustered into n_j regions. Let v_i be $i-th$ input pixel of image and c_j is the $j-th$ cluster (centre) ($i = 1, 2, 3, \ldots, N, j = 1, 2, 3, \ldots, n_j$). Based on original Moving K-means clustering algorithm [12], the algorithm of using the Moving K-means clustering to find the clusters values can be implemented as:

1 Initialize the centers and α_0, set $\alpha_0 = \alpha_a = \alpha_b$, (where α_0 is a small constant value, $0 < \alpha_0 < \frac{1}{3}$ and should be chosen to be inversely proportional to the number of centre).

2 Assign all pixels to the nearest cluster and calculate the center position using (2).

$$C_j = \frac{1}{n_j} \sum_{i \in C_j} \left(\| v_i - C_j \| \right)^2 \tag{2}$$

3 Check the fitness of each center using (3).

$$f\left(C_j\right) = \sum_{i \in C_j} \left(\| v_i - C_j \| \right)^2 \tag{3}$$

4 Find C_s and C_l, the cluster that has the smallest and the largest value of $f(\cdot)$.

5 If $f(C_s) < \alpha_a f(C_l)$

5.1 Assign the pixels of C_l to C_s if $v_i < C_l$ and $i \in C_l$ and leave the rest of the pixels to C_l.

5.2 Recalculate the positions of C_s and C_l according to

$$\begin{aligned} C_s &= \frac{1}{n_s} \sum_{i \in C_s} v_i \\ C_l &= \frac{1}{n_l} \sum_{i \in C_l} v_i \end{aligned} \tag{4}$$

Note: C_s will give up its pixels before step (5.1) and, n_s and n_l in (2) are the number of the new pixels of C_s and C_l respectively, after the reassigning process in step (5.1).

6 Update α_a according to $\alpha_a = \alpha_a - \frac{\alpha_a}{n_j}$ and repeat step (4) and (5) until $f(C_s) \geq \alpha_a f(C_l)$

7 Reassign all pixels to the nearest centre and recalculate the centre positions using (2).

8 Update α_a and α_b according to $\alpha_a = \alpha_b$ and $\alpha_a = \alpha_b - \frac{\alpha_b}{n_j}$ respectively, and repeat step (3) to (7) until $f(C_s) \geq \alpha_b f(C_l)$

9 Sort the centres in ascending order where $C_1 < C_2 < \cdots < C_{n_j}$

In blood cells images segmentation, Moving K-means clustering will segment the images into three main structures of acute leukemia cells, which are background, nucleus and cytoplasm. In other words, the output from the Moving K-means clustering is the pixels value that have been clustered in three regions $n_j = 3$ as shown in Figure 3(d) to 10(d). Cluster for background, nucleus and cytoplasm represented by C_1, C_2 and C_3, respectively. After completing the segmentation process, the output of Moving K-means clustering is filtered by using 7×7 pixels median filter to improve the segmented images.

2.2.3. Removing Unwanted Noise

The 7×7 pixels median filter is further applied to the segmented images in order remove unwanted noise. This process yields better and more acute leukemia blood cells image visualization.

2.2.4. Image Segmentation Evaluation

The performance of the proposed image segmentation technique is evaluated using subjective and supervised evaluation. Subjective evaluation is referring to human visual inspection by comparing the resultant segmented images with the results from other segmentation algorithm [19]. Meanwhile, the supervised evaluation is another common evaluation in which a segmented image will be compared against a manually segmented image [19]. Pixel subtraction technique is used for evaluating the proposed image segmentation technique. The pixel subtraction technique takes two images as inputs that are the resultant segmented image and manual segmented image. Then, produces as output a third image whose pixel values are those of the first image minus the corresponding pixel values from the second image. Manual segmented images were prepared manually by editing the images using Adobe PhotoshopTM. The segmentation performance of Moving K-means and K-means algorithms is evaluated based on the percentage accuracy of correct segmentation of pixels, as follows;

$$Accuracy(\%) = \frac{TP + TN}{TP + TN + FN + FP} \times 100\% \tag{5}$$

where TP, TN, FP and FN are true positive, true negative, false positive and false negative, respectively.

3. RESULTS AND DISCUSSIONS

The proposed method was applied on 200 images of acute leukemia, which were taken from 6 slides of acute leukemia blood samples. Figure 3(a) to 10(a) show the original captured acute leukemia images with resolution of 800x600. Figure 3(a) to 6(a) show the original AML images while Figure 7(a) to 10(a) show the original ALL images. Both types of acute leukemia original images can be differentiated through the description of shape and size of the cells. Figure 3(b) to 10(b) show the resultant images after applying saturation formula base on HSI color space. The results obtained in Figures 3(b) to 10(b) show that resultant images of the proposed method by beginning with applying the saturation formula to AML and ALL original images to ease the clustering process.

From Figure 3(d) to 6(d) for AML images, as well as Figure 7(d) to 10(d) for ALL images, it can be noticed that Moving K-means clustering algorithm has successfully clustered the regions of interest for the acute leukemia images to three regions, which are background, nucleus and cytoplasm. From Figure 3(d) to 10(d), a 7x7 pixels median filter is applied to the resultant images produced by the Moving K-means algorithm to give better results. Figure 3(h), 5(h), 6(h), 8(h), 9(h) and 10(h) show that the unwanted noise (portions of red blood cells) regions are detected as part of the regions of interest using K-means clustering procedures. However, less of the unwanted noise regions are detected using Moving K-means clustering procedures as shown in Figure 3(e), 4(e), 5(e), 6(e), 7(e) and 8(e).

With reference to original acute leukemia images in Figure 3(a) to 10(a), the segmented blasts in Figure 3(e) to 10(e) retain the size and give the almost similar shape. Results of pixel subtraction technique between the manually segmented images and the resultant segmented images in are shown in Figure 3(f) to 10(f) and 3(i) to 10(i) for moving K-means clustering and K-means clustering, respectively. From Figure 3(f) to 10(f) and 3(i) to 10(i), the ghost images that represent the unsuccessfully segmented object appeared in original colour. Therefore, Figure 3(f) to 10(f) and 3(i) to 10(i) indicate that the proposed method is successful to retain the blasts shape. Generally, Moving K-means clustering produced better performance as compared to K-means clustering algorithm,

although some problems were still not totally avoided (e.g. some small portions of red blood cells in ALL images still appear) as shown in Figure 9(e) and 10(e).

Table 1 and 2 summarized the segmentation performance using Moving K-means and K-means clustering algorithm. The percentage of accuracy is calculated based on comparison of the pixels that represent resultant segmented image and the pixels represent manual segmented image. The number of data used for testing is 492681 pixels that is equivalent to the size image, which is 809×609. From the result obtained, segmentation using Moving K-means procedures produced better performance with 98.00%, 99.35%, 98.92% (for AML1, AML3 and AML4 images) and 99.13%, 98.07%, 94.24% (for ALL2, ALL3 and ALL4 images).

As compared to K-means clustering procedures, which are 85.02%, 84.24%, 84.12% for AML images and 94.63%, 86.08%, 87.30% for ALL images, respectively. However, by referring to Figure 4(d)AML2 and 7(d)ALL1, the performance accuracy are 99.54% and 98.27% by using Moving K-means algorithm compare against the resultant image from K-means algorithm with performance accuracy are 99.57% and 98.34%, respectively. The results show that Moving K-means clustering algorithm do not all the time produce better performance than k-means clustering but the performance is always good.

The percentage of accuracy as in (6) is calculated based on comparison of the pixels that represent the resultant segmented image and the pixels represent manual segmented image. If the test correctly indicates the blasts (object of interest), then the pixels that represent the blasts are counted as true positive (TP). If the test correctly indicates, the pixels that represent the background or red blood cells, then it will be counted as true negative (TN). However, if the test falsely indicates the blasts when truly is, then it will be counted as false negative (FN). Finally, if the test falsely indicates the pixels that represent the background or red blood cells, it will be counted as false positive (FP).

4. CONCLUSIONS

The current study proposed an image segmentation technique consists of saturation component base on HSI colour space, Moving K-means algorithm and 7×7 pixels median filter procedures. The saturation component is chosen as an input features for the Moving K-means clustering. 7×7 pixels median filter were further applied in order to eliminate and remove unwanted noise. The advantage of the proposed method is that the selection of the threshold for segmentation is done automatically. The pixels subtraction technique is used in order to evaluate the performance accuracy of the proposed image segmentation technique. The results indicated that the acute leukemia cells in the blood slide images are successfully segmented from its background and unwanted noise. Furthermore, the size and shape of the acute leukemia cells are closely preserved.

ACKNOWLEDGMENT

We would like to express our thanks to UniMAP and Malaysian Government for supporting this research in term of research grant. This research is funded under Fundamental Research Grant Scheme (Grant No. 9003 00129).

REFERENCES

1. Mittal, P. and Meehan, K.R., "The Acute Leukemia", *Clinical Review Article, Hospital Physician* , 37–44, 2001.
2. World Health Organization (WHO) Report 2009, "The Global Burden of Disease: 2004 update", 2009.
3. Altekruse, S.F., Kosary, C.L., Krapcho, M., Neyman, N., Aminou, R., Waldron, W., Ruhl, J., Howlader, N., Tatalovich, Z., Cho, H., Mariotto, A., Eisner, M.P., Lewis, D.R.,

Cronin, K., Chen, H.S., Feuer, E.J., Stinchcomb, D.G. and Edwards, B.K. (eds). "SEER Cancer Statistics Review", 1975-2007, National Cancer Institute. Bethesda, MD, http://seer.cancer.gov/csr/1975_2007/, based on November 2009 SEER data submission, posted to the SEER web site, 2010.

4. Panovska-Stavridis, I., Cevreska, L., Trajkova, S., Hadzi-Pecova, L., Trajkov, D., Petlichkovski, A., Efinska-Mladenovska, O., Sibinovska, O., Matevska, N., Dimovski, A. and Spiroski, M. "Preliminary Results of Introducing the Method Multiparameter Flow Cytometry in Patients with Acute Leukemia in the Republic of Macedonia", *Maced J Med Sci.* , 36–43, 2008.
5. Schumacher, H.R. and Cotelingam, J.D. *Chronic monocytic leukemia. Case #7"* . In: Chronic leukemia: Approach to diagnosis, New York, NY. Igaku-Shoin, 261–268, 1993.
6. Piuri, V. and Scotti, F. "Morphological classification of blood leucocytes by microscope images", *In Proceedings of the International Conference in Computational Intelligence for Measurement Systems and Applications* , 103–108, 2004.
7. Venkateswaran, N. and Ramana Rao, Y.V. "K-means Clustering Based Image Compression in Wavelet Domain", *Journal of Information Technology* , 148–153, 2007.
8. Chen, C.W., Luo, J. and Parker, K.J. "Image Segmentation via Adaptive K-Mean Clustering and Knowledge-Based Morphological Operations with Biomedical Applications", *IEEE Transactions on Image Processing* , 1673–1683, 1998.
9. Pham, D., Prince, J.L., Chen, Y.X. and Dagher, A.P. "An Automated Technique for Statistical Characterization of Brain Tissues in Magnetic Resonance Imaging", *International Journal of Pattern Recognition and Artificial Intelligence* , 1189–1211, 1997.
10. Wu, M.N., Lin, C.C. and Chang, C.C. "Brain tumor detection using color based K-means clustering", *In 3rd International Conference Intelligent Information Hiding and Multimedia Signal Processing* , 245–250, 2007.
11. Etahad-Tavakol, M, Sadri, S. and Ng, E.Y.K. "Application of K- and Fuzzy c-Means for Color Segmentation of Thermal Infrared Breast Images", *In Journal Medical System* , 2008.
12. Mashor, M.Y. "Hybrid Training Algorithm for RBF network", *International Journal of the Computer,The Internet and Management* , 50–65, 2000.
13. Mat-Isa, N.A., Mashor, M.Y. and Othman, N.H. "Comparison of Segmentation Performance of Clustering Algorithms for Pap Smear Images", *In International Conference on Robotics, Vision, Information and Signal Processing* , 118–125, 2003.
14. Mat-Isa, N.A. "Automated Edge Detection Technique for Pap Smear Images Using Moving K-Means Clustering and Modified Seed Based Region Growing Algorithm", *International Journal of The Computer, the Internet and Management* 45–59, 2005.
15. Mat-Isa, N.A., Sabaruddin, S., Ngah, U.K. Zamli, K.Z. and Noor, M.M. "The Potential Use of Modified Seed Based-Region Growing Technique for Automatic Detection of Breast Microcalcifications and Tumor Areas", *Jurnal Teknologi, UTM* , 151–164, 2006.
16. Harun, N.H., Mashor, M.Y., Mokhtar, N.R., Abdul-Nasir, A.R., Hassan, R., Raof, R.A.A. and Osman, M.K. "Comparison of Acute Leukemia using HSI and RGB color space" *In 10th International Conference on Information Science, Signal Processing and their Applications (ISSPA 2010)* , 740–752, 2010.
17. Gonzalez, R.C. and Woods, R.E. *Digital Image Processing* , 3ed: Prentice Hall, 2007.
18. Osman, M.K., Mashor, M.Y., Saad, Z. and Jaafar, H. "Color Image Segmentation of Ziehl-Neelsen-Stained Tissue Images using Moving K-Mean Procedure" *In 2010 Fourth Asia International Conference on Mathematical Analytical Modelling and Computer Simulation* , 215–219, 2010.
19. Zhang, H., Fritts, J.E. and Goldman, S.A. "Image Segmentation: A survey of unsupervised methods", *In Journal Computer Vision and Image Understanding* , 260–280, 2008.

Table 1: Segmentation performance of clustering algorithm for AML type

(a) AML1 type					
Clustering algorithm	Accuracy %	True Positive	True Negative	False Positive	False Negative
K-means	85.02%	48541	370356	2570	71214
Moving K-means	98.00%	41281	441548	9830	22
(b)AML2 type					
Clustering algorithm	Accuracy %	True Positive	True Negative	False Positive	False Negative
K-means	99.57%	14796	475774	1908	203
Moving K-means	99.54%	14623	475810	2081	167
(b)AML3 type					
Clustering algorithm	Accuracy %	True Positive	True Negative	False Positive	False Negative
K-means	84.24%	29057	386025	76941	658
Moving K-means	99.35%	26735	462727	239	2980
(b)AML4 type					
Clustering algorithm	Accuracy %	True Positive	True Negative	False Positive	False Negative
K-means	84.12%	31004	383376	769777	1324
Moving K-means	98.92%	27193	460151	202	5135

Table 2: Segmentation performance of clustering algorithm for ALL type

(a) ALL1 type					
Clustering algorithm	Accuracy %	True Positive	True Negative	False Positive	False Negative
K-means	98.34%	39384	444179	8004	31
Moving K-means	98.27%	39387	444812	8451	164
(b)ALL2 type					
Clustering algorithm	Accuracy %	True Positive	True Negative	False Positive	False Negative
K-means	94.63%	20952	445306	3119	23304
Moving K-means	99.13%	19843	46856	4228	49
(a) ALL3 type					
Clustering algorithm	Accuracy %	True Positive	True Negative	False Positive	False Negative
K-means	86.08%	29347	394763	67842	729
Moving K-means	98.07%	27635	455562	7043	2441
(b)ALL4 type					
Clustering algorithm	Accuracy %	True Positive	True Negative	False Positive	False Negative
K-means	87.30%	38654	391481	61143	1403
Moving K-means	94.24%	36295	428017	24607	3762

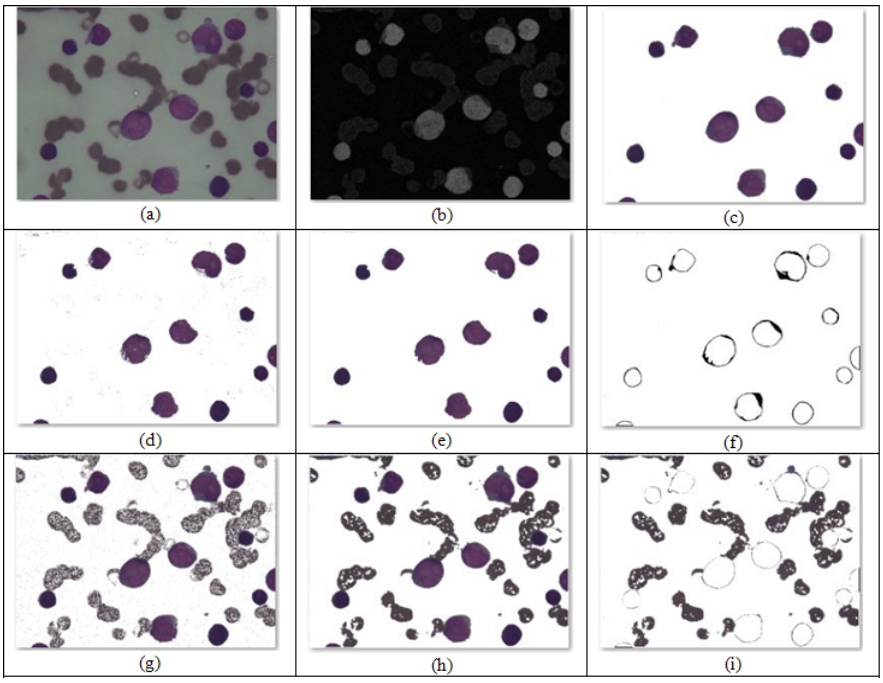

Figure 3: Resulted images for AML1 (a) original image (b) saturation component resulted image (c) manual segmented image (d) Moving K-means resulted image (e) 7x7 median filter resulted image (f) Ghost Image (g) K- mean clustering resulted image(h) 7x7 median filter resulted image (i) Ghost Image

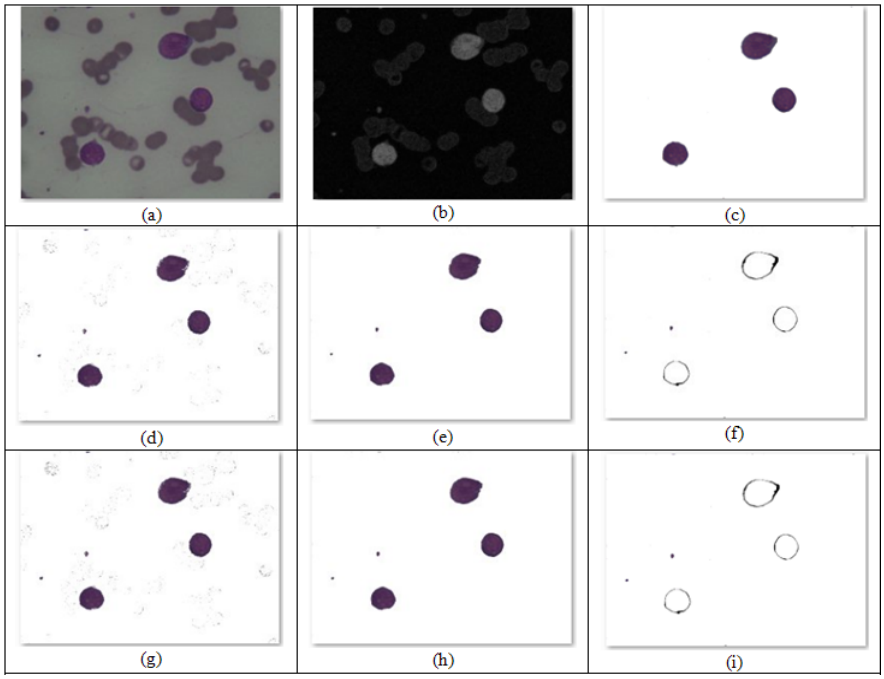

Figure 4: Resulted images for AML2 (a) original image (b) saturation component resulted image (c) manual segmented image (d) Moving K-means resulted image (e) 7x7 median filter resulted image (f) Ghost Image (g) K- mean clustering resulted image(h) 7x7 median filter resulted image (i) Ghost Image

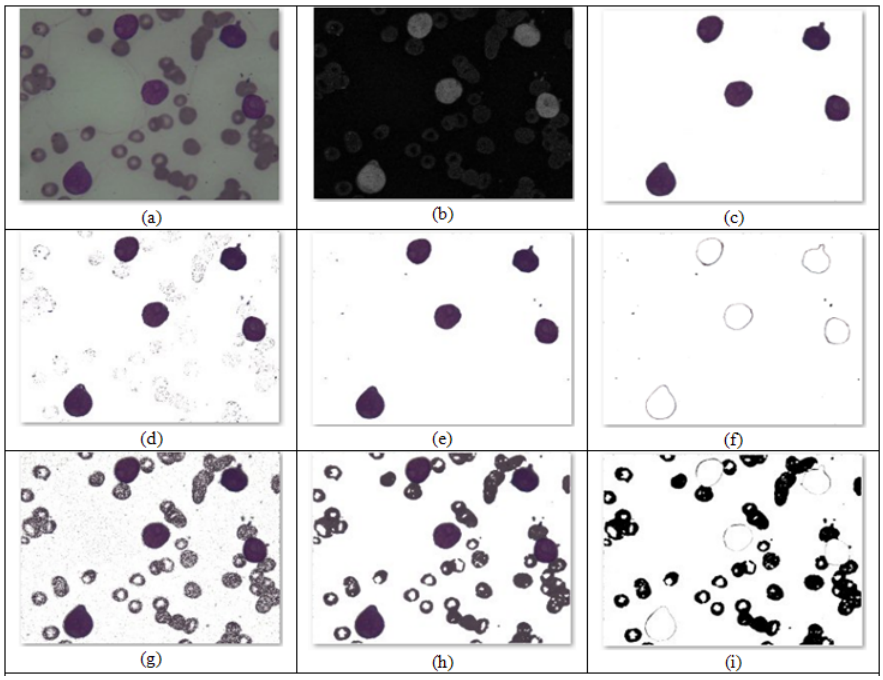

Figure 5: Resulted images for AML3 (a) original image (b) saturation component resulted image (c) manual segmented image (d) Moving K-means resulted image (e) 7x7 median filter resulted image (f) Ghost Image (g) K- mean clustering resulted image(h) 7x7 median filter resulted image (i) Ghost Image

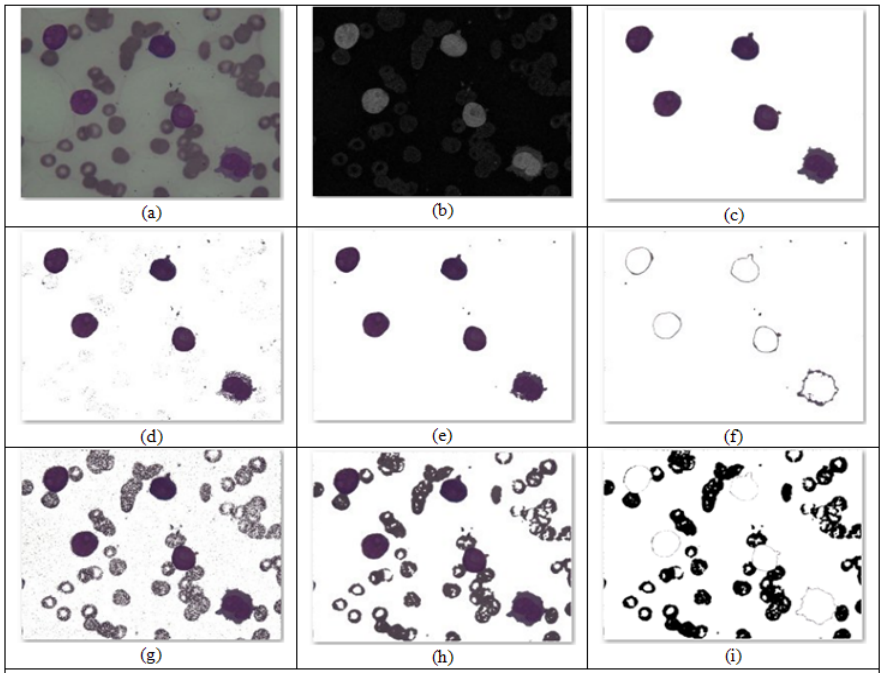

Figure 6: Resulted images for AML4 (a) original image (b) saturation component resulted image (c) manual segmented image (d) Moving K-means resulted image (e) 7x7 median filter resulted image (f) Ghost Image (g) K- mean clustering resulted image(h) 7x7 median filter resulted image (i) Ghost Image

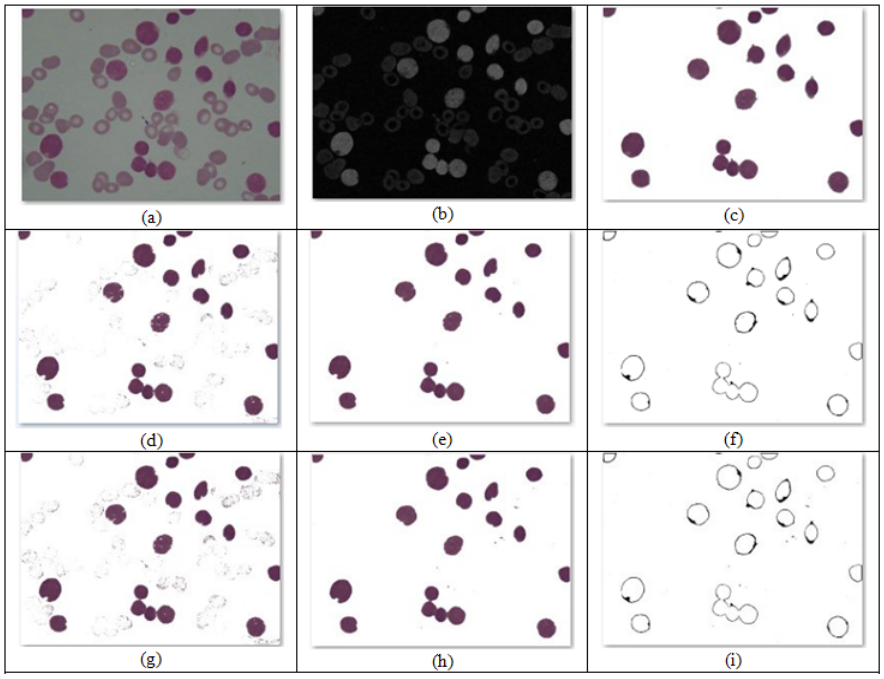

Figure 7: Resulted images for ALL1 (a) original image (b) saturation component resulted image (c) manual segmented image (d) Moving K-means resulted image (e) 7x7 median filter resulted image (f) Ghost Image (g) K- mean clustering resulted image(h) 7x7 median filter resulted image (i) Ghost Image

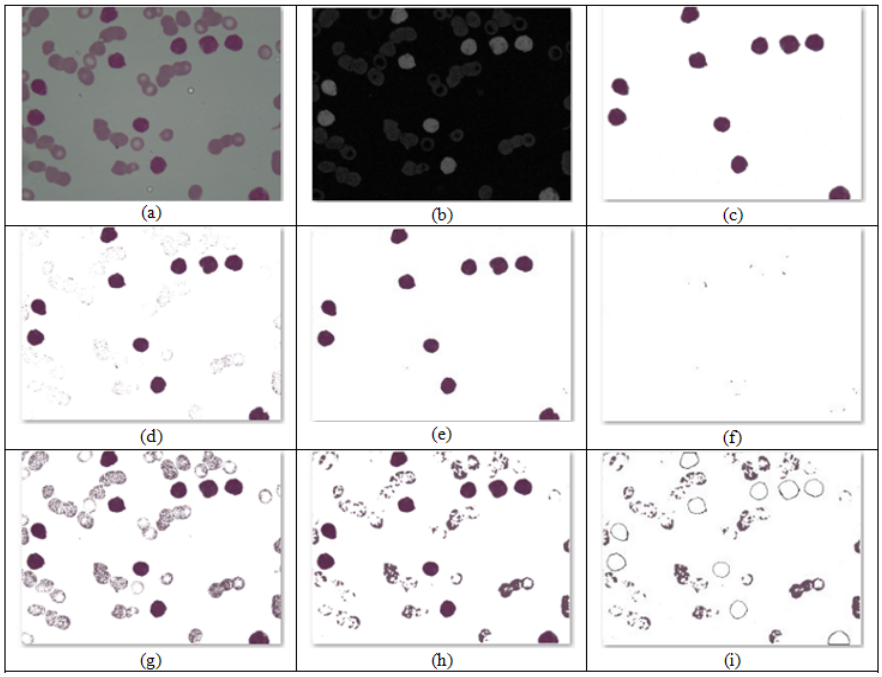

Figure 8: Resulted images for ALL2 (a) original image (b) saturation component resulted image (c) manual segmented image (d) Moving K-means resulted image (e) 7x7 median filter resulted image (f) Ghost Image (g) K- mean clustering resulted image(h) 7x7 median filter resulted image (i) Ghost Image

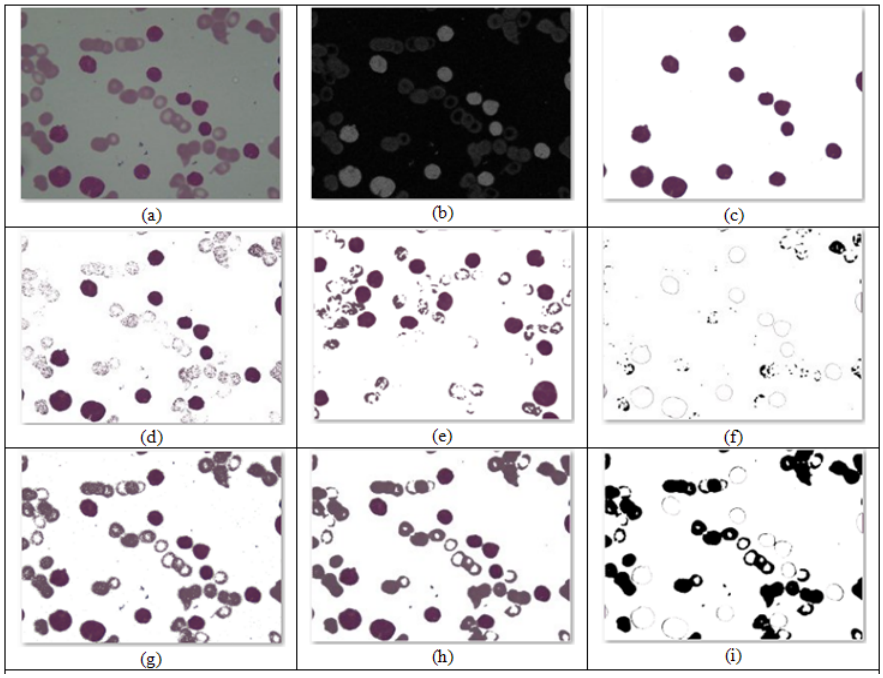

Figure 9: Resulted images for ALL3 ((a) original image (b) saturation component resulted image (c) manual segmented image (d) Moving K-means resulted image (e) 7x7 median filter resulted image (f) Ghost Image (g) K- mean clustering resulted image(h) 7x7 median filter resulted image (i) Ghost Image

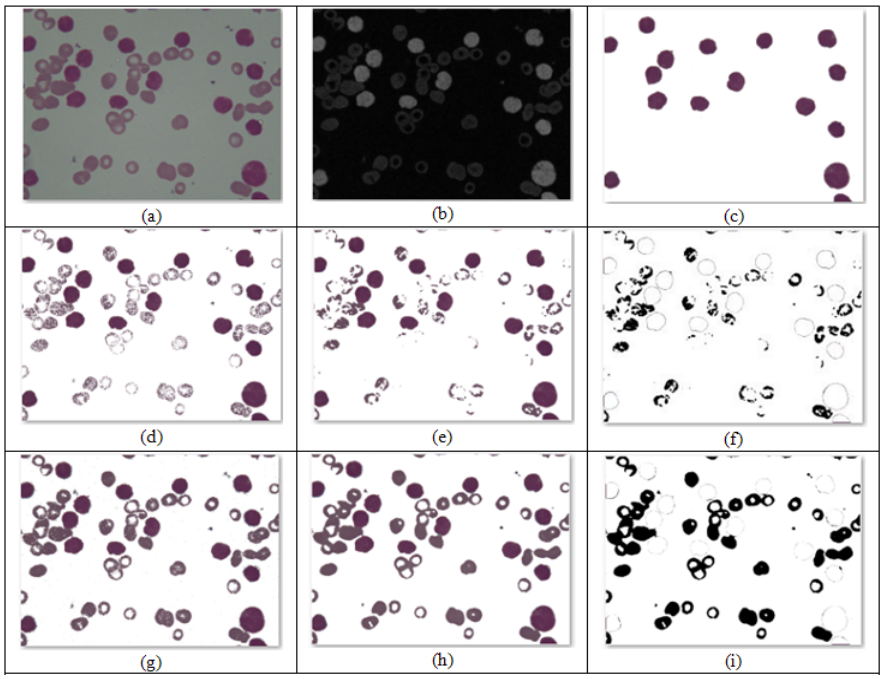

Figure 10: Resulted images for ALL4 (a) original image (b) saturation component resulted image (c) manual segmented image (d) Moving K-means resulted image (e) 7x7 median filter resulted image (f) Ghost Image (g) K- mean clustering resulted image(h) 7x7 median filter resulted image (i) Ghost Image